MOLECULAR AND CELLULAR BIOLOGY, Apr. 1987, p. 1393–1400
0270-7306/87/041393-08$02.00/0

Vol. 7, No. 4

Target Sequences for *cis*-Acting Regulation within the Dual Promoter of the Human c-*myc* Gene

MARTIN LIPP,[1]* RENATE SCHILLING,[1] SIEGLINDE WIEST,[2] GERHARD LAUX,[2] AND GEORG W. BORNKAMM[2]

Institut für Biochemie der Universität München, D-8000 Munich 2,[1] and Institut für Virologie, Zentrum für Hygiene der Universität Freiburg, D-7800 Freiburg,[2] Federal Republic of Germany

Received 10 March 1986/Accepted 17 December 1986

Recombinant plasmids of the human c-*myc* promoter-leader region and the bacterial chloramphenicol acetyltransferase (*cat*) gene were constructed. After transfection into different rodent and human cells, the 862-base-pair (bp) *Pvu*II fragment carrying both c-*myc* promoters and 350 bp of the untranslated leader conferred 1/15 to 1/30 of the CAT activity mediated by the simian virus 40 promoter. The presence of additional sequences upstream of the *Pvu*II fragment had an overall negative effect on c-*myc* promoter activity detectable by titration analysis with small amounts of transfected plasmid DNA. The analysis of numerous deletion constructs in the c-*myc* promoter-leader region as well as S1 mapping experiments demonstrated that the high CAT activity depended largely on the presence of the second promoter. By cotransfection of c-*myc-cat* constructs with plasmids carrying different parts of the c-*myc* promoter locus, targets for positively acting cellular factors were identified. Two positive regulatory elements were mapped within the 862-bp *Pvu*II fragment. One was localized within the 248-bp *Pvu*II-*Sma*I fragment −101 to −349 bp upstream of the first cap site and the other within the 142-bp *Xho*I-*Nae*I fragment of the first exon, comprising positions −95 to +47 relative to the second cap site. We conclude that the dual promoter of the human c-*myc* gene represents a strong eucaryotic promoter regulated by cooperation of positively and negatively acting cellular transcription factors.

The c-*myc* gene, the cellular counterpart of the oncogene of the avian retrovirus MC29 (13), appears to play an important role in normal cell proliferation. In response to exogenous stimuli such as platelet-derived growth factor in fibroblasts and lectin or anti-immunoglobulin M in lymphocytes, c-*myc* mRNA is accumulated about 2 to 3 h after induction, prior to the onset of cellular DNA synthesis (1, 22, 26). The c-*myc* gene is composed of three exons, the first of which is noncoding (5, 6, 19, 38). Transcription of the c-*myc* gene proceeds from two initiation sites (P_1 and P_2) 160 base pairs (bp) apart from each other at the beginning of the first exon. The human c-*myc* gene codes for a protein with a predicted molecular weight of 48,000 (48K protein) (5, 6, 17, 37, 38). However, two proteins of 64 and 67K, located in the nucleus, were shown to be coded for by the c-*myc* gene. Their function is not yet understood (20, 27).

Perturbations of the c-*myc* gene have been shown to occur in many B-cell malignancies in chicken, mice, and humans (for a review, see reference 23). In many cases of Burkitt's lymphomas with the t(8;14) and mouse plasmacytomas with the t(12:15) translocation which involve the heavy-chain locus, the chromosomal translocations disrupt the first exon or the first intron of the c-*myc* gene and thus separate the body of the gene from its physiological promoters, possibly causing deregulated transcription of the c-*myc* gene from otherwise cryptic promoters (2, 6, 21, 33, 34). In cases with the variant translocations t(2:8) and t(8:22), which involve the kappa or lambda light-chain genes, the breakpoint is usually far downstream of the c-*myc* gene, leaving the c-*myc* transcription unit intact (9, 11, 15, 30). Multiple somatic mutations in the first exon have been described in three cases in which the breakpoint does not disrupt the c-*myc* gene (28, 29, 34). It is not known whether generation of somatic mutations is a general mechanism leading to deregulation of the c-*myc* gene in cells with variant translocations. Mechanisms operating at a posttranscriptional level also seem to play an important role in the regulation of the c-*myc* gene (10, 26).

To determine the target structures of the c-*myc* gene required for transcriptional and posttranscriptional regulation, we have constructed hybrid molecules containing part of the c-*myc* promoter-leader region and the bacterial chloramphenicol acetyltransferase (CAT) gene (*cat*). The activity of the fused genes was tested after transfection into various cell types. With a number of deletion constructs, positively and negatively *cis*-acting regulatory sequences were identified. Also, by cotransfection experiments of c-*myc-cat* constructs with plasmids carrying different parts of the c-*myc* locus, target sequences for positively acting cellular factors were determined.

Our work demonstrates that the c-*myc* promoter-leader region efficiently drives the synthesis of CAT in various human and rodent cells and that the second of the two promoters is particularly important for the activity of the constructs. The dual promoter of the human c-*myc* gene represents a strong eucaryotic promoter regulated by the cooperation of positively and negatively acting cellular factors.

MATERIALS AND METHODS

Construction of hybrid molecules of the human c-*myc* and *cat* gene. To construct pmycCAT-P, the 12.5-kilobase (kb) *Eco*RI fragment carrying the hyman c-*myc* gene was cloned from the normal allele of the Burkitt's lymphoma line Raji in the phage EMBL4 (16) and subcloned into the *Eco*RI site of pUC12. The 862-bp *Pvu*II fragment was subcloned into the *Sma*I site of pUC12. A clone was selected which had the *Bam*HI, *Xba*I, and *Hin*dIII sites of the polylinker down-

* Corresponding author.

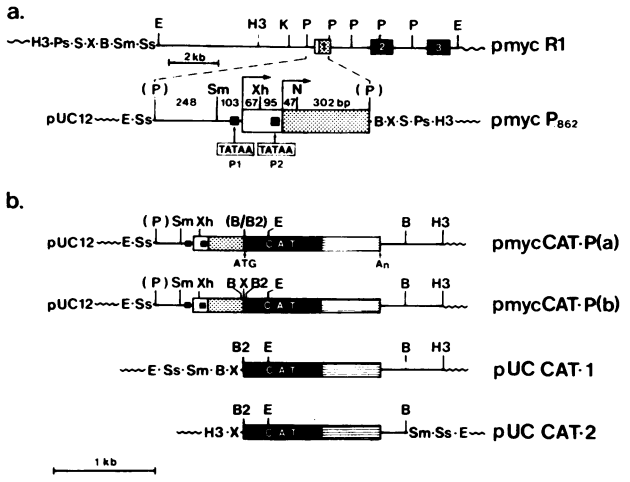

FIG. 1. Schematic representation of constructed hybrid molecules of the human c-*myc* and the bacterial *cat* genes. Blocks designate possible transcribed regions, solid blocks indicate the coding sequences of the expressed gene, arrows show the normal transcriptional start sites, lined blocks indicate the SV40-derived splice and polyadenylation sites, and solid boxes designate the presumptive Hogness-Goldberg signals (TATAA). (a) The 12.5-kb *Eco*RI fragment carrying the human c-*myc* gene was subcloned into the *Eco*RI site of pUC12 (pmycR1). The 862-bp *Pvu*II fragment containing both c-*myc* promoters (P_1 and P_2) and most of the noncoding first exon was subcloned in the *Sma*I site of pUC12 ($pmycP_{862}$). (b) Hybrid molecules of the human c-*myc* 862-bp *Pvu*II fragment and the bacterial *cat* gene (pmycCAT-P). Wavy lines designate pUC12 sequences. Abbreviations: B, *Bam*HI; B2, *Bgl*II; E, *Eco*RI; H3, *Hin*dIII; K, *Kpn*I; N, *Nae*I; Ps, *Pst*I; P, *Pvu*II; S, *Sal*I; Sm, *Sma*I; Ss, *Sst*I; X, *Xba*I; Xh, *Xho*I. Restriction sites shown in parentheses were lost.

stream of the promoters and the first exon ($pmycP_{862}$). DNA from this clone was double digested with *Bam*HI and *Hin*dIII or with *Xba*I and *Hin*dIII, and the large fragments were isolated by preparative gel electrophoresis with NA45 paper (Schleicher & Schüll). DNA of the plasmid CAT3M (24) was digested with *Bgl*II, *Hin*dIII, and *Pst*I or with *Xba*I, *Hin*dIII, and *Pst*I, and the fragments carrying the *cat* gene were isolated. The *Bgl*II-*Hin*dIII and *Xba*I-*Hin*dIII fragments carrying the *cat* gene were ligated into the isolated *Bam*HI-*Hin*dIII and *Xba*I-*Hin*dIII fragments of the clone containing the promoters and the first exons to generate pmycCAT-P(a) (*Bam*HI/*Bgl*II-*Hin*dIII) and pmycCAT-P(b) (*Xba*I-*Hin*dIII) (Fig. 1). To delete sequences from pmycCAT-P, the deletion constructs pmycCAT-S, pmycCAT-X, pmycCAT-PΔN, pmycCAT-XΔN, pmycCAT-PΔP1, and pmycCAT-PΔP2 were obtained by digestion with appropriate restriction enzymes, followed by religation.

For reinsertion of upstream sequences, pmycCAT-P(a) and (b) were double-digested with *Sac*I and *Xho*I, and the large fragments were isolated. Similarly, a clone containing the 12.5-kb *Eco*RI fragment in pUC12 in the appropriate orientation was digested with *Sac*I and *Xho*I, and the fragment containing the upstream region and the first promoter of the c-*myc* gene was isolated from the gel. The fragments were ligated to generate pmycCAT-R1(a) and (b). From this clone the deletion constructs pmycCAT-B2, pmycCAT-Sp, and pmycCAT-K were obtained by digestion with *Sac*I and *Bgl*II, *Spe*I, and *Kpn*I, respectively, followed by religation. A derivative without the second promoter, pmycCAT-R1ΔP2, was prepared by digestion of pmycCAT-R1(b) with *Xho*I and *Xba*I, followed by religation. The different constructs used in this study are schematically shown in Fig. 1 and 3D.

Cells. All recipient cells used in transfection experiments were grown at 37°C with 5% CO_2 in Dulbecco modified Eagle medium supplemented with 5% fetal calf serum. The cell lines were obtained originally from the indicated investigators or companies: baby hamster kidney (BHK) cells (G. Brandner, Freiburg); mouse L cells (Flow Laboratories, Glasgow); 143tk$^-$ cells (S. Bacchetti, Hamilton [4]).

Transfection of eucaryotic cells. Transfection with 20 μg of superhelical plasmid DNA per 10^6 cells in 9-cm tissue culture dishes by the calcium phosphate coprecipitation technique was done as described by Schöler and Gruss (31). In the titration experiments, pUC12 was used as carrier DNA to yield a total amount of 20 μg of DNA per plate.

Assay for CAT activity. Published procedures were followed (18) to assay CAT activity, with a few minor modifications. At 44 h after transfection cells were harvested, suspended in 150 μl of 0.25 M Tris hydrochloride buffer (pH 7.8), and sonicated twice for 5 s each. Then 100 to 600 μg of protein, corresponding to about 20 to 150 μl of the clarified cell extract, was incubated with 20 μl of 4 mM acetyl coenzyme A (P-L Biochemicals) and 0.2 to 0.4 μCi of [^{14}C]chloramphenicol (CAM) (50 μCi/ml, 57.8 mCi/mmol; New England Nuclear Corp.) in 0.25 M Tris hydrochloride buffer (pH 7.8) at a final volume of 175 μl for 1 h at 37°C. The ^{14}C-labeled CAM was extracted two times with 400 μl of ethyl acetate, dried, suspended in 20 μl of ethyl acetate, and spotted to a thin-layer silica gel plate (0.25 mm; Merck). The two spots which corresponded to the monoacetylated forms of CAM were simultaneously measured with a thin-layer scanner (Berthold), and the total amount of ^{14}C-acetyl-CAM was calculated from the area under the resulting peak.

S1 mapping. Total cellular RNA was prepared 40 h after transfection by the urea-lithium cloride method (3). S1 nuclease analysis of this RNA was performed with a ^{32}P-labeled single-stranded DNA probe obtained by primer extension reaction with M13 DNA in the presence of 100 μCi of [α-^{32}P]dCTP (410 Ci/mmol; Amersham) at 20°C for 1 h. The RNA samples (30 to 50 μg) were coprecipitated with the isolated single-stranded probe fragment (about 10^5 cpm), suspended in 20 μl of hybridization buffer (40 mM PIPES [piperazine-*N*-*N*′-bis(2-ethanesulfonic acid, pH 6.5], 400 mM NaCl, 1 mM EDTA, 90% formamide), heated at 95°C for 5 min, and hybridized overnight in a water bath at 56°C. Then 180 μl of ice-cold S1 buffer (30 mM sodium acetate, pH 4.5, 250 mM NaCl, 2.5 mM zinc acetate) containing 4×10^3 U of S1 nuclease (Boehringer Mannheim) was added, and the mixture was incubated at 37°C for 1 h. The S1-resistant hybrids were precipitated and analyzed on a 5% sequencing gel.

Sequencing. The nucleotide sequence of the 862-bp *Pvu*II fragment of the c-*myc* gene which was cloned originally from the normal, not translocated allele of Raji cells was determined by the method of Maxam and Gilbert (25) and showed no deviation from the c-*myc* sequence published by Gazin et al. (17).

RESULTS

c-*myc* promoter active in various cell lines in vitro. The activity of the c-*myc* promoter was analyzed in titration experiments in which the amount of pmycCAT-P DNA (for construction of pmycCAT-P, see Fig. 1), used for transient transfection, was plotted against the resulting CAT activity.

Because of its universal expression in all cells tested so far, the simian virus 40 (SV40) promoter was used as an internal standard. pmycCAT-P and pSV2CAT had very different titration curves (Fig. 2). In all three cell lines tested, the higher activity of the SV40 promoter was much more clearly apparent when small amounts of DNA were used for transfection. The activity of the two promoters was compared quantitatively by comparing the CAT activities mediated by equimolar nonsaturating amounts of DNA and also by comparing the amounts of DNA required for half-maximal CAT activity. The half-logarithmic plots shown in the lower panels of Fig. 2 are designed to facilitate the determination of the amount of DNA required for half-maximal activity. From these data it became apparent that the c-*myc* promoter was 15-fold, 20-fold, and 30-fold less active than the SV40 promoter in BHK cells, mouse L cells, and the human permanent fibroblast line 143tk$^-$ cells, respectively.

Second promoter of c-*myc* mainly responsible for the high CAT activity. In an attempt to identify the sequences required for activity and regulation of the c-*myc* promoter, we tested the activities of the various constructs shown in Fig. 3D. These were designed in relation to the location of DNase I-hypersensitive sites in the upstream and promoter regions of the c-*myc* gene (14, 32, 36). In addition to the construct, pmycCAT-P (−511 bp relative to the cap site of P_2, deletion of DNase I-hypersensitive sites I, II_1, and II_2), recombinant plasmids were tested by titration analysis in BHK cells, in which various parts of the 862-bp *Pvu*II fragment were deleted (Fig. 3A). pmycCAT-S (−263 bp, deletion of site III_1) exhibited a lower activity than pmycCAT-P. Deletion of another 170 bp containing the first promoter (P_1) in the construct pmycCAT-X (−95 bp) had no influence on the CAT activity. Deletions of 3′ sequences of the first exon downstream from the *Nae*I site in the construct pmycCAT-XΔN (−95 to +47) had no apparent effect on the activity of the construct compared with pmycCAT-X (Fig. 3A). This plasmid, pmycCAT-XΔN, comprising positions −95 to +47 relative to the cap site of the second promoter (P_2) and containing DNase I-hypersensitive site III_2), conferred most of the CAT activity. Removal of this 142-bp *Xho*I-*Nae*I fragment and the noncoding sequences downstream from pmycCAT-P, generating the constructs pmycCAT-PΔX-N (Δ−95 to +47) and pmycCAT-PΔP2 (Δ−95), respectively, decreased the activity dramatically (five- to sixfold). In contrast, removal of the 170-bp *Sma*I-*Xho*I fragment carrying P_1 (pmycCAT-PΔP1, Δ−263 to −95) increased the resulting CAT activity (Fig. 3A). Comparison of the constructs lacking P_1 or P_2 revealed at least six- to eightfold-higher activity of the plasmid carrying the second promoter. The relative CAT activities of the different constructs compared with that of pmycCAT-P are indicated in Fig. 3D. The mean values calculated from repeated titration analysis correspond to 0.5 to 1.0 pmol of transfected DNA.

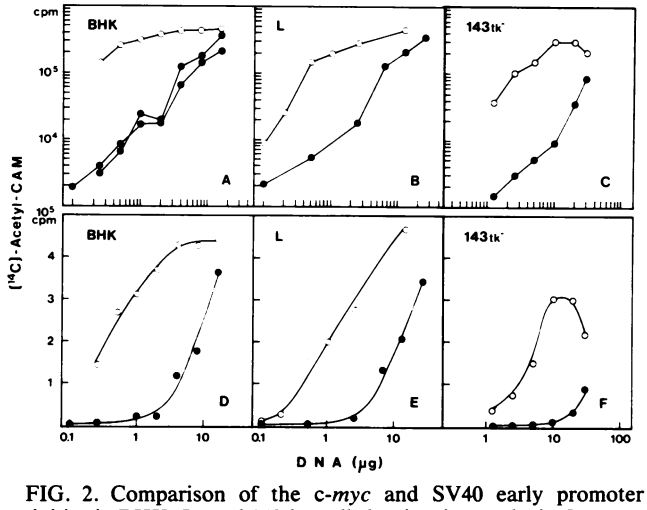

FIG. 2. Comparison of the c-*myc* and SV40 early promoter activities in BHK, L, and 143tk$^-$ cells by titration analysis. Increasing amounts of pmycCAT-P (●) and pSV2CAT (○) were transfected into subconfluent BHK (A and D), L (B and E), and 143tk$^-$ (C and F) cells. CAT activity was determined with 350 μg (BHK and L) or 500 μg (143tk$^-$) of protein of the prepared cell extract and plotted against the logarithm of transfected test DNA (in micrograms). (A, B, and C) Double logarithmic representation was used to demonstrate, at low input of transfected DNA, the approximately linear relationship between CAT activity and amount of DNA used. The half-logarithmic plots shown in the lower panels (D, E, and F) facilitate the determination of the amount of test DNA required for half-maximal CAT activity.

Evidence for regulatory elements further upstream of the c-*myc* promoter. We examined whether sequences upstream of the c-*myc* promoters carried elements modulating the promoter activity. CAT activity mediated by pmycCAT-P (−511 bp) was therefore compard with that of pmycCAT-R1 (−6,900 bp), pmycCAT-B2 (−2,950 bp), pmycCAT-Sp (−1,560 bp, deletion of DNase I-hypersensitive site I), and pmycCAT-K (−1,220 bp, deletion of sites I and II_1). With higher amounts of transfected DNA (more than 0.52 pmol), slightly lower but similar activity was obtained with the long constructs pmycCAT-R1, -B2, and -Sp (Fig. 3A and C). However, with lower amounts of transfected DNA (in the range of 0.026 to 0.52 pmol, corresponding to 0.1 to 2.0 μg in the case of pmycCAT-P), the observed CAT activity diverged significantly. As shown in the double logarithmic plot in Fig. 3C, the long construct, pmycCAT-R1, revealed two- to eightfold lower activity than the short pmycCAT-P plasmid. This suggests that a negative regulatory element might be located upstream of the *Pvu*II site. To localize the regions which are responsible for the reduced activity, we performed a comparative titration analysis of pmycCAT-P, -Sp, and -K in BHK cells (Fig. 3A) and human fibroblasts (Fig. 3B). In the range of 0.5 to 1.0 pmol of transfected DNA, pmycCAT-Sp showed intermediate CAT activity (about 50 to 60% of pmycCAT-P activity). With pmycCAT-K, in which 340 bp from pmycCAT-Sp were deleted, the activity decreased significantly (10 to 20%). This result could indicate that the reduced CAT activity observed with the long *myc-cat* constructs was caused by the simultaneous effect of a positive and a negative element (Fig. 3D). Similar to the short plasmid pmycCAT-PΔP2, removal of the second promoter from pmycCAT-R1ΔP2 decreased the CAT activity considerably (Fig. 3C). This suggests that the upstream sequences cannot activate P_1 significantly during transient expression.

Hybrid c-*myc-cat* RNAs initiate correctly at the c-*myc* promoters. We asked then whether transcription of the c-*myc-cat* hybrids was correctly initiated. S1 analysis of RNA from transfected BHK cells was carried out with a single-stranded probe spanning the first exon. With RNA from cells transfected by pmycCAT-R1, pmycCAT-P, pmycCAT-S, pmycCAT-X, and pmycCAT-PΔP1, a prominent band with a length of 350 bp was protected (Fig. 4). This 350-bp long fragment corresponded to RNA initiated at the second c-*myc* promoter. Transcripts starting at the first promoter should protect a fragment of 510 bases. Only a faint band of this size was seen after transfection of pmycCAT-R1, pmycCAT-P, and pmycCAT-S, indicating that the

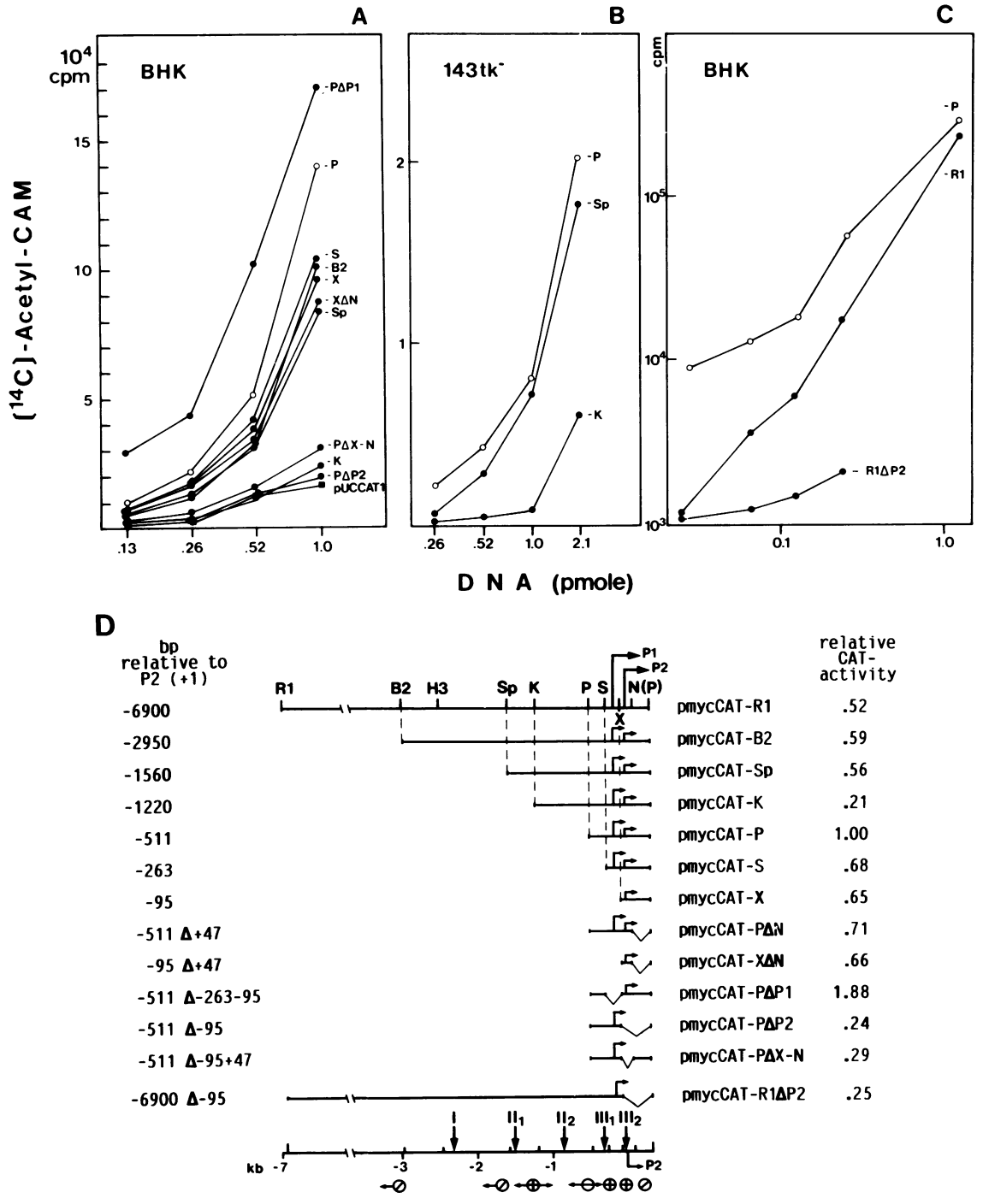

FIG. 3. Comparison of the CAT activity mediated by different constructs of the c-*myc* promoter region. Increasing equimolar amounts of the various *cat* constructs, described in detail in panel D and the legend to Fig. 1, were transfected into BHK (A and C) and 143tk$^-$ (B) cells. Levels of CAT activity were determined with 100 μg (A) or 500 μg (B) of protein of the prepared cellular extract. (C) CAT activity determined from 200 μg of protein was plotted in a double logarithmic representation to demonstrate the deviation in CAT activity at low input of transfected DNA (0.263 pmol of pmycCAT-P DNA [P] = 1 μg). (D) Schematic representation of the c-*myc*-specific sequences present in the various CAT constructs. For further details see Materials and Methods and Fig. 1. The length (in base pairs) of the upstream sequences and the positions of the deletions are indicated relative to P_2. The relative CAT activities of the different constructs compared with that of pmycCAT-P are indicated. The mean values were calculated from repeated titration analysis and correspond to 0.5 to 1.0 pmol of transfected DNA. The lower part of the scheme shows the location of the proposed DNase I-hypersensitive sites (32) and the regions of regulatory elements which confer a positive (+), a negative (−), or no measurable (/) effect on c-*myc* promoter activity. Abbreviations: R1, *Eco*RI; B2, *Bgl*II; H3, *Hin*dIII; Sp, *Sph*I; K, *Kpn*I; P, *Pvu*II; S, *Sma*I; N, *Nae*I; X, *Xho*I. Restriction site in parentheses was lost.

second promoter is used much more efficiently. The bands with a size of 615 and 450 bases were generated by the transfected plasmid DNAs contaminating the RNA preparation. This was shown by digestion with DNase I in the presence of RNase inhibitor (data not shown). The results of the S1 assays correspond to the different levels of CAT expression obtained by titration analysis (Fig. 3), demonstrating that the RNA is correctly initiated at the sites also used in vivo.

Expression of pmyc-CAT constructs in stable transfected cells. We considered it important to ask whether the differences in the CAT activity of certain pmyc-CAT plasmids seen after transient expression would be identical or similar after stable integration into the chromatin of cells. BHK cells were therefore cotransfected with the individual pmyc-CAT constructs and pSVneo and selected for G418 resistance without isolating individual cell clones (to normalize for different integration sites). About 8 weeks after transfection, cellular extracts were prepared and their CAT activities were determined. In the stable transfectants the same pattern of CAT activity was obtained as in transient expression assays (Fig. 5). Cells carrying pmycCAT-P and pmycCAT-R1 had identical CAT activity (100%). Integration of pmycCAT-S and pmycCAT-X resulted in moderate enzyme activity (62 to 81%). Deletion of the first promoter (pmycCAT-PΔP1) stimulated the activity in stably transfromed cells as well (192%), whereas deletion of the second promoter (pmycCAT-PΔP2) decreased expression of the CAT gene significantly (39%).

Sequences around the c-*myc* promoters compete for cellular transcription factors. Evidence for two positively acting elements within the 862-bp *Pvu*II-*Pvu*II fragment had already been obtained from the experiments shown in Fig. 3,

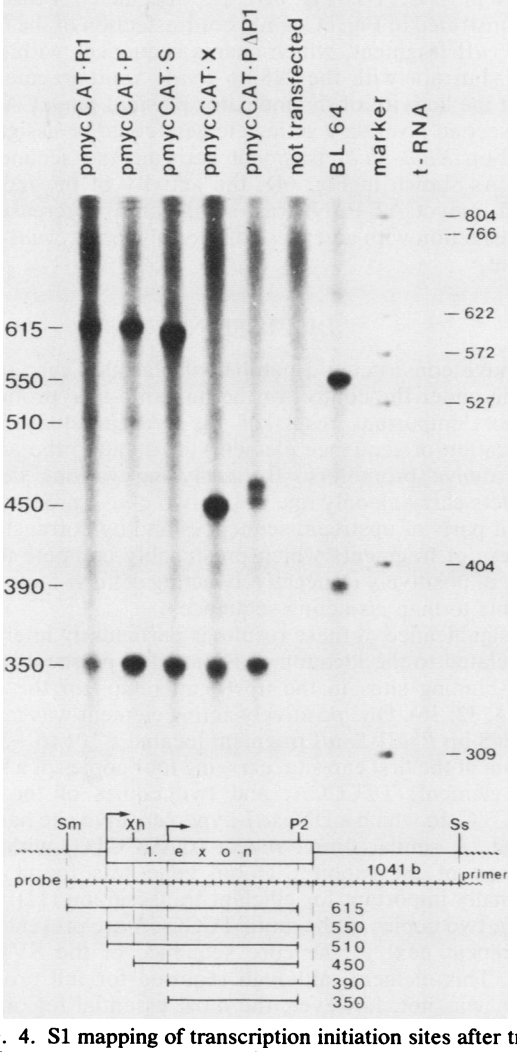

FIG. 4. S1 mapping of transcription initiation sites after transfer of various c-*myc*-*cat* constructs into BHK cells. A single-stranded 1,041-base *Sst*I-*Sma*I probe from the c-*myc* first exon region was hybridized to 40 μg of BHK RNA isolated 40 h after transfection with the indicated c-*myc*-*cat* plasmids to 20 μg of RNA of the Burkitt's lymphoma cell line BL64 [t(2;8)] and to 10 μg of tRNA, digested with S1 nuclease, and analysed on a 5% sequencing gel. In the diagrammatic representation below the autoradiograph, a scheme of the M13 clone used and of the size and the location of the S1 nuclease-protected fragments is shown. Arrows indicate the two sites of mRNA initiation. The bands with a size of 615 and 450 bases (b) were generated by the transfected plasmid DNAs contaminating the RNA preparations. The double band observed in lane five is probably due to the formation of a secondary structure. The abbreviations for restriction enzymes are as used in Fig. 1.

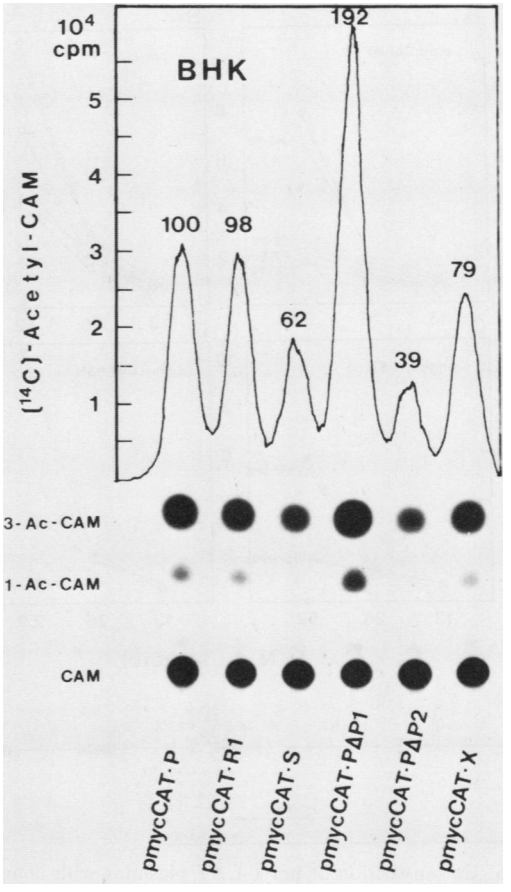

FIG. 5. Expression of pmyc-CAT constructs in biochemically transformed BHK cells. BHK cells were cotransfected with equimolar amounts of pmyc-CAT constructs (10 μg for pmycCAT-P) and pSVneo (1 μg) and selected for G418 (400 μg/ml) resistance. Cells of one petri dish of each transfection experiment were propagated without isolating individual cell clones. About 8 weeks after transfection, cellular extracts were prepared and the CAT activity was determined with 400 μg of protein. The CAT activity of the different cell lines was compared with the activity of cells biochemically transformed by pmycCAT-P and is expressed as a percentage above the individual peaks.

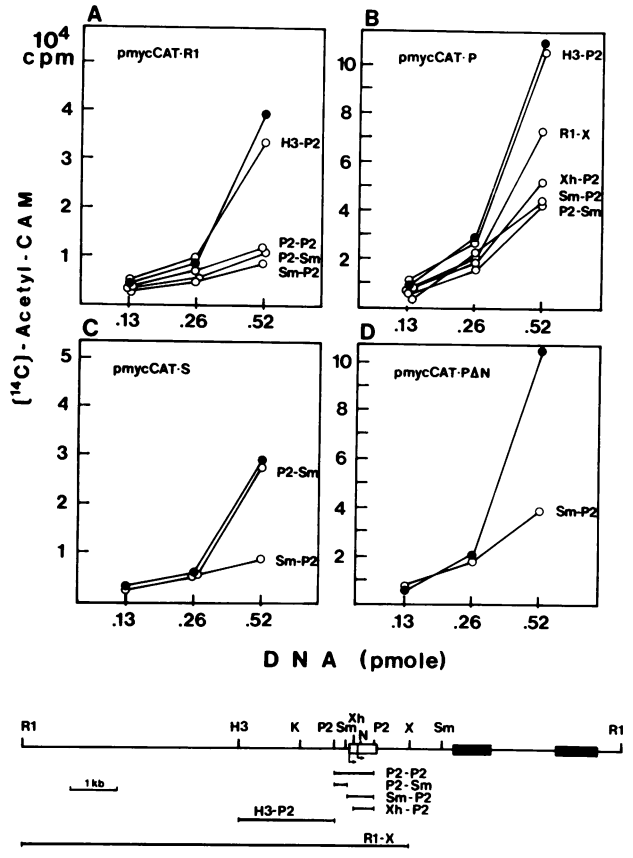

FIG. 6. Cotransfection of pmyc-CAT plasmids with competitor DNAs. Increasing amounts of pmyc-CAT indicator plasmids were transfected in the presence of constant amounts of competitor DNAs into subconfluent BHK cells. Because of the relatively low expression of pmyc-CAT constructs at low concentrations of transfected DNA and because of the limited amount of about 20 μg of DNA which can be used in one transfection experiment, the amount of competitor and not of indicator plasmid was kept constant. The CAT activity was determined 32 to 36 h after transfection with 400 μg of protein of the cellular extract. The following indicator plasmids were used: A, pmycCAT-R1; B, pmycCAT-P (1 μg = 0.263 pmol); C, pmycCAT-S; and D, pmycCAT-PΔN. The titration kinetics of the indicator plasmids in the absence of competitor DNA and the presence of carrier DNA are indicated with solid circles. The competitor plasmids, carrying the fragments shown in the scheme below and next to the individual titration curves, were used in 5 to 10 molar excess with respect to the highest concentration of the indicator plasmid. The CAT activities in the presence of competitor plasmids are symbolized with open circles.

in which deletions of the 248-bp upstream *Pvu*II-*Sma* fragment as well as of the second promoter reduced the activity of the *myc-cat* constructs considerably. These observations were confirmed and extended in cotransfection experiments in which pmycCAT-R1, pmycCAT-P, pmycCAT-S, and pmycCAT-PΔN as indicator plasmids were cotransfected with an excess of subcloned fragments carrying possible target sites for negatively or positively interacting cellular factors. Cotransfection of pmycCAT-R1 (Fig. 6A) and pmycCAT-P (Fig. 6B) with the 2.0-kb *Hin*dIII-*Pvu*II upstream fragment did not alter the CAT activity, as expected for pmycCAT-P, which has no sequences in common with the cotransfected fragment. However, for pmycCAT-R1 this result indicates that cellular factors possibly binding to the negatively and positively modulating elements upstream of the *Pvu*II site cannot be titrated out, leading to activation or inhibition of the promoter activity.

A significant inhibitory effect was observed when pmycCAT-R1 as the indicator plasmid was cotransfected with the 862-bp *Pvu*II-*Pvu*II fragment carrying both promoters, the 248-bp *Pvu*II-*Sma*I fragment upstream of the first promoter, or the 614-bp *Sma*I-*Pvu*II fragment with both promoters (Fig. 6A). Both fragments upstream and downstream of the *Sma*I site, the 450-bp *Xho*I-*Pvu*II fragment carrying the second promoter and the 8.0-kb *Eco*RI-*Xba*I fragment containing the complete first exon, showed a similar inhibitory effect on pmycCAT-P (Fig. 6B). The specificity of this effect is demonstrated in Fig. 6C. Only cotransfection of the 614-bp *Sma*I-*Pvu*II fragment, which shares sequences with pmycCAT-S, but not with the 248-bp *Pvu*II-*Sma*I fragment decreased the activity of the indicator plasmid pmycCAT-S.

The second positively acting element could be assigned to the 142-bp *Xho*I-*Nae*I fragment carrying the second promoter. As shown in Fig. 6D, the activity of the indicator plasmid pmycCAT-PΔN was significantly decreased by contransfection with an excess of the subcloned *Sma*I-*Pvu*II fragment.

DISCUSSION

We have constructed a number of plasmids carrying the *cat* gene under the control of the human c-*myc* promoters. The most important result of the present study is the identification of sequence elements modulating the activity of the c-*myc* promoters. By analyzing various deletion constructs carrying only one of the two c-*myc* promoters or different parts of upstream sequences and by cotransfecting an excess of fragments which presumably compete for the binding of positively or negatively acting cellular factors, we were able to map *cis*-acting sequences.

The significance of these results is particularly interesting when related to the location of DNase I-hypersensitive and protein-binding sites in the upstream region of the c-*myc* gene (14, 32, 36). One positively acting element was mapped to the 248-bp *Pvu*II-*Sma*I fragment located −101 to −349 bp upstream of the first cap site, carrying four copies of a simple repeat element, TCCCCA, and two copies of the motif CACCCTC, to which a DNase I-hypersensitive site has been assigned. A similar direct repeat (CACCCTG) within the −100 box of the rabbit β-globin gene was found to be functionally important for efficient transcription (12). Interestingly, two copies of the motif TCCCCA are present in the 72-bp repeat next to the core sequence of the SV40 enhancer. This element, although required for full promoter activity, was not, however, the most essential region. The promoter activity was more dramatically reduced when sequences downstream of the *Xho*I site were deleted. This second positive element could be assigned to the 142-bp *Xho*I-*Nae*I fragment (position −95 to +47), which carries the second promoter. In contrast, deletion of the 170-bp *Sma*I-*Xho*I fragment carrying the first promoter (pmycCAT-PΔP1) led to an increase in promoter activity. It thus appears that the region carrying the first promoter is negatively modulating overall c-*myc* promoter activity. However, we were unable to compete for a negatively regulating factor by using the *Sma*I-*Xho*I fragment in cotransfection experiments (data not shown). Thus, alternatively, the higher activity of pmycCAT-PΔP1 than of pmycCAT-P may be the result of the juxtaposition of the two DNase I-hypersensitive sites

which are located in front of each c-*myc* promoter. This could also explain the slightly reduced activity of pmycCAT-S and pmycCAT-X.

By analyzing the activity of 5′ deletion mutants, evidence accumulated for negative and positive regulatory elements. Interestingly, the putative positively *cis*-acting element which is located upstream of the negative element can compensate for the negative effect. We were not able to identify both modulating elements simply by cotransfection experiments with the upstream *Hin*dIII-*Pvu*II fragment. An explanation might be that both effects neutralize each other or that the entire binding domain of the negative factor is not present on this fragment. On the other hand, we think that the location of these elements does not coincide exactly with the DNase I-hypersensitive sites II_1 and II_2 (Fig. 3D), because nuclear factor I (NfI)-binding sites proposed to be responsible for these sites (32) are not conserved beween humans and mice (8). Thus, the exact location and function of these upstream regulatory elements cannot be concluded from this study and remain to be elucidated by further fine-mapping with additional deletion constructs.

Our finding that the c-*myc* promoter carries target structures for positively acting transcription factors is in line with recently published data showing that the level of c-*myc* mRNA is invariant throughout the cell cycle (35) and that the c-*myc* gene is transcribed at a high rate in G0-arrested Chinese hamster lung fibroblasts without detectable mature mRNA in the cytoplasm (7). Since after stimulation with growth factors the level of cytoplasmic c-*myc* mRNA increased without alteration of the transcription rate, the authors proposed a model of posttranscriptional regulation of c-*myc* expression. However, neither study distinguished the usage of the individual cap sites. Our S1 mapping data clearly demonstrate that the second promoter is used almost exclusively during transient expression. This appears to reflect at least in part the situation in vivo, in which the second promoter is used more efficiently for transcription of the normal c-*myc* gene (34). It should be pointed out that no sequence homology could be found between consensus binding sequences of any known eucaryotic transcription factor and the 142-bp *Xho*I-*Nae*I fragment which confers the high CAT activity of the pmyc-CAT constructs.

Interestingly, the pmyc-CAT constructs carrying the first promoter mediated only very little CAT activity in monolayer cells as well as in B cells (unpublished observation) in transient expression assays. This promoter is preferentially used in vivo in most Burkitt's lymphoma cells (see Fig. 4 for the BL64 line). With c-*myc-cat* constructs from the nontranslocated c-*myc* allele of Raji cells, we were unable to activate the first promoter either with deletion mutants or by cotransfection. One possibility is that elements driving transcription from the first promoter are located upstream or downstream of the sequences present in the various *cat* constructs. Alternatively, the preferential use of the first promoter might be a special feature of altered c-*myc* genes. As a third possibility, the different promoter use might reflect a peculiar chromatin structure in vivo which is not formed when exogenous DNA is transiently or stably introduced into the cells.

With the experimental approach described here, it will be possible to study in more detail the interaction of the c-*myc* gene with the cellular factors modulating c-*myc* expression. It will be of particular importance to see whether the promoters of the c-*myc* genes derived from the normal or translocated chromosome of Burkitt's lymphoma show functional differences in transient expression assays and differences in their ability to interact with cellular regulating factors.

ACKNOWLEDGMENTS

We thank I. Kruczek for providing us with the construct pSV2CAT and P. Gruss for gift of pCAT3M. We are particularly grateful to D. Eick for help with the S1 experiments and for providing the M13 probe. We thank H. Synovzik for excellent technical assistance and E. L. Winnacker for critically reading the manuscript.

The work was supported by the Deutsche Forschungsgemeinschaft (Li 374/1-1 and SFB 31, Medizinische Virologie: Tumorentstehung und Entwicklung).

LITERATURE CITED

1. **Armelin, H. A., M. C. S. Armelin, K. Kelly, T. Stewart, P. Leder, B. H. Cochran, and C. D. Stiles.** 1984. Functional role for c-*myc* in mitogenic response to platelet-derived growth factor. Nature (London) **310**:655–660.
2. **Ar-Rushdi, A., K. Nishikura, J. Erikson, R. Watt, G. Rovera, and C. M. Croce.** 1983. Differential expression of the translocated and the untranslocated c-*myc* oncogene in Burkitt's lymphoma. Science **222**:390–393.
3. **Auffray, C., and F. Rougeon.** 1980. Purification of mouse immunoglobulin heavy-chain messenger RNA's from total myeloma tumor RNA. Eur. J. Biochem. **107**:303–314.
4. **Bacchetti, S., and F. L. Graham.** 1977. Transfer of the gene for thymidine kinase to thymidine kinase-deficient human cells by purified herpes simplex viral DNA. Proc. Natl. Acad. Sci. USA **74**:1590–1594.
5. **Battey, J., C. Moulding, R. Taub, W. Murphy, T. Stewart, H. Potter, G. Lenoir, and P. Leder.** 1983. The human c-*myc* oncogene: structural consequences of translocation into the IgH locus in Burkitt's lymphoma. Cell **34**:779–787.
6. **Bernard, O., S. Cory, S. Gerondakis, E. Webb, and J. M. Adams.** 1983. Sequence of the murine and human cellular *myc* oncogenes and two modes of *myc* transcription resulting from chromosome translocation in B lymphoid tumours. EMBO J. **2**:2375–2383.
7. **Blanchard, J.-M., M. Piechaczyk, C. Dani, J.-C. Chambard, A. Franchi, J. Pouyssegur, and P. Jeanteur.** 1985. c-*myc* gene is transcribed at high rate in G_0-arrested fibroblasts and is posttranscriptionally regulated in response to growth factors. Nature (London) **317**:443–445.
8. **Corcoran, L. M., S. Cory, and J. M. Adams.** 1985. Transposition of the immunoglobulin heavy chain enhancer to the *myc* oncogene in a murine plasmacytoma. Cell **40**:71–79.
9. **Croce, C. M., W. Thierfelder, J. Erikson, K. Nishikura, J. Finan, G. M. Lenoir, and P. C. Nowell.** 1983. Transcriptional activation of an unrearranged and untranslocated c-*myc* oncogene by translocation of a C-lamda locus in Burkitt's lymphoma cells. Proc. Natl. Acad. Sci. USA **80**:6922–6926.
10. **Dani, C., J. M. Blanchard, M. Piechaczyk, S. El Sabouty, L. Marty, and P. Jeanteur.** 1984. Extreme instability of *myc* mRNA in normal and transformed human cells. Proc. Natl. Acad. Sci. USA **81**:7046–7050.
11. **Davis, M., S. Malcolm, and T. H. Rabbitts.** 1984. Chromosome translocation can occur on either side of the c-*myc* oncogene in Burkitt's lymphoma cells. Nature (London) **308**:286–288.
12. **Dierks, P., A. Van Ooyen, M. D. Cochran, C. Dobkin, C. Reiser, and C. Weissmann.** 1983. Three regions upstream from the CAP site are required for efficient and accurate transcription of the rabbit beta-globin gene in mouse 3T6 cells. Cell **32**:695–706.
13. **Duesberg, P. H., K. Bister, and C. Moscovici.** 1980. Genetic structure of avian myeloblastosis virus, released from transformed myeloblasts as a defective virus particle. Proc. Natl. Acad. Sci. USA **77**:5120–5124.
14. **Dyson, P. J., and T. H. Rabbitts.** 1985. Chromatin structure around the c-*myc* gene in Burkitt's lymphomas with upstream and downstream translocation points. Proc. Natl. Acad. Sci. USA **82**:1984–1988.
15. **Erikson, J., K. Nishikura, A. Ar-Rushdi, J. Finan, B. Emanuel,**

G. Lenoir, P. C. Nowell, and C. M. Croce. 1983. Translocation of an immunoglobulin kappa-locus to a region 3′ of an unrearranged c-*myc* oncogene enhances c-*myc* transcription. Proc. Natl. Acad. Sci. USA **80**:7581–7585.

16. **Frischauf, A.-M., H. Lehrach, A. Poustka, and N. Murray.** 1983. Lamda replacement vectors carrying polylinker sequences. J. Mol. Biol. **170**:827–842.
17. **Gazin, C., S. Dupont De Dinechin, A. Hampe, J.-M. Masson, P. Martin, D. Stehelin, and F. Galibert.** 1984. Nucleotide sequence of the human c-*myc* locus: provocative open reading frame within the first exon. EMBO J. **3**:383–387.
18. **Gorman, C. M., L. F. Moffat, and B. H. Howard.** 1982. Recombinant genomes which express chloramphenicol acetyltransferase in mammalian cells. Mol. Cell. Biol. **2**:1044–1051.
19. **Hamlyn, P. H., and T. H. Rabbitts.** 1983. Translocation joins c-*myc* and immunoglobulin gamma-1 genes in a Burkitt's lymphoma revealing a third exon in the c-*myc* oncogene. Nature (London) **304**:135–139.
20. **Hann, S. R., and R. N. Eisenman.** 1984. Proteins encoded by the human c-*myc* oncogene: differential expression in neoplastic cells. Mol. Cell. Biol. **4**:2486–2497.
21. **Hayday, A. C., S. D. Gillies, H. Saito, C. Wood, K. Wiman, W. S. Hayward, and S. Tonegawa.** 1984. Activation of a translocated human c-*myc* gene by an enhancer in the immunoglobulin heavy-chain locus. Nature (London) **307**:334–340.
22. **Kelly, K., B. H. Cochran, C. D. Stiles, and P. Leder.** 1983. Cell-specific regulation of the c-*myc* gene by lymphocyte mitogens and platelet-derived growth factor. Cell **35**:603–610.
23. **Klein, G.** 1983. Specific chromosomal translocations and the genesis of B-cell-derived tumors in mice and men. Cell **32**:311–315.
24. **Laimins, L. A., P. Gruss, R. Pozzatti, and G. Khoury.** 1984. Characterization of enhancer elements in the long terminal repeat of Moloney murine sarcoma virus. J. Virol. **49**:183–189.
25. **Maxam, A. M., and W. Gilbert.** 1977. A new method for sequencing DNA. Proc. Natl. Acad. Sci. USA **74**:560–564.
26. **McCormack, J. E., V. H. Pepe, R. B. Kent, M. Dean, A. Marshak-Rothstein, and G. E. Sonenshein.** 1984. Specific regulation of c-*myc* oncogene expression in a murine B-cell lymphoma. Proc. Natl. Acad. Sci. USA **81**:5546–5550.
27. **Persson, H., and P. Leder.** 1984. Nuclear localization and DNA binding properties of a protein expressed by human c-*myc* oncogene. Science **225**:718–721.
28. **Rabbitts, T. H., A. Forster, P. Hamlyn, and R. Baer.** 1984. Effect of somatic mutation within translocted c-*myc* genes in Burkitt's lymphoma. Nature (London) **309**:592–597.
29. **Rabbitts, T. H., P. H. Hamlyn, and R. Baer.** 1983. Altered nucleotide sequences of a translocated c-*myc* gene in Burkitt's lymphoma. Nature (London) **306**:760–765.
30. **Rappold, G. A., H. Hameister, T. Cremer, S. Adolph, B. Henglein, U.-K. Freese, G. M. Lenoir, and G. W. Bornkamm.** 1984. c-*myc* and immunoglobulin kappa light chain constant genes are on the $8q^+$ chromosome of three Burkitt's lymphoma lines with t(2;8) translocation. EMBO J. **3**:2951–2955.
31. **Schöler, H. R., and P. Gruss.** 1984. Specific interaction between enhancer-containing molecules and cellular components. Cell **36**:403–411.
32. **Siebenlist, U., L. Hennighausen, J. Battey, and P. Leder.** 1984. Chromatin structure and protein binding in the putative regulatory region of the c-*myc* gene in Burkitt's lymphoma. Cell **37**:381–391.
33. **Stanton, L. W., R. Watt, and K. B. Marcu.** 1983. Translocation, breakage and truncated transcripts of c-*myc* oncogene in murine plasmacytomas. Nature (London) **303**:401–406.
34. **Taub, R., C. Moulding, J. Battey, W. Murphy, T. Vasicek, G. M. Lenoir, and P. Leder.** 1984. Activation and somatic mutation of the translocated c-*myc* gene in Burkitt's lymphoma cells. Cell **36**:339–348.
35. **Thomson, C. B., P. B. Challoner, P. E. Neiman, and M. Groudine.** 1985. Levels of c-*myc* oncogene mRNA are invariant throughout the cell cycle. Nature (London) **314**:363–366.
36. **Tuan, D., and I. M. London.** 1984. Mapping of DNase I-hypersensitive sites in the upstream DNA of human embryonic epsilon-globin gene in K562 leukemia cells. Proc. Natl. Acad. Sci. USA **81**:2718–2722.
37. **Watson, D. K., M. C. Psallidopoulos, K. P. Samuel, R. Dalla-Favera, and T. S. Papas.** 1983. Nucleotide sequence analysis of human c-*myc* locus, chicken homologue, and myelocytomatosis virus MC29 transforming gene reveals a highly conserved gene product. Proc. Natl. Acad. Sci. USA **80**:3642–3645.
38. **Watt, R., K. Nishikura, J. Sorrentino, A. Ar-Rushdi, C. M. Croce, and G. Rovera.** 1983. The structure and nucleotide sequence of the 5′ end of the human c-*myc* oncogene. Proc. Natl. Acad. Sci. USA **80**:6307–6311.